



Contents lists available at ScienceDirect

Quaternary Science Reviews

journal homepage: www.elsevier.com/locate/quascirev

Micromammal and macromammal stable isotopes from a MIS 6 fossil hyena den (Pinnacle Point site 30, south coast, South Africa) reveal differences in relative contribution of C₄ grasses to local and regional palaeovegetation on the Palaeo-Agulhas Plain

Hope M. Williams^a, Julia A. Lee-Thorp^b, Thalassa Matthews^c, Curtis W. Marean^{d, e, *}

^a School of Human Evolution and Social Change, PO Box 872402, Arizona State University, Tempe, AZ, 85287-2402, USA

^b Research Laboratory for Archaeology and the History of Art, School of Archaeology, University of Oxford, 1-2 South Parks Road, Oxford, OX1 3TG, United Kingdom

^c Centre of Excellence for Palaeontology, Iziko Museums of South Africa, 25 Queen Victoria Street, Cape Town 8000, South Africa

^d African Centre for Coastal Palaeoscience, Nelson Mandela University, Port Elizabeth, Eastern Cape, 6031, South Africa

^e Institute of Human Origins, School of Human Evolution and Social Change, PO Box 872402, Arizona State University, Tempe, AZ, 85287-2402, USA

ARTICLE INFO

Article history:

Received 29 October 2019

Received in revised form

27 January 2020

Accepted 28 January 2020

Available online xxx

Keywords:

Africa

South Africa

Cape floral region

Palaeo-Agulhas plain

Pleistocene

Marine isotope stage 6

Micromammal

Macromammal

Radiogenic isotopes

ABSTRACT

Proxy records dating to marine isotope stage 6 on the south coast of South Africa are rare. This study presents integrated micromammal and macromammal stable isotope palaeoenvironmental proxy data from one of the few MIS 6 fossil occurrences in the region, a fossil brown hyena (*Parahyena brunnea*) den, Pinnacle Point 30 (PP30). Two predators with significantly different foraging ranges aggregated the large and small mammal components of the PP30 fossil assemblage. The large mammal specimens were brought to PP30 by *Parahyena brunnea* with an expansive daily foraging radius that focused on the Palaeo-Agulhas Plain. The micromammal taxa were deposited at the site primarily by the spotted eagle owl, *Bubo africanus*, with a foraging radius of ~3 km, and would have sampled the ecotone between the Palaeo-Agulhas Plain and the Cape coastal lowlands. The large and small mammal components of the PP30 assemblage thus sample palaeovegetation at different geographic scales; micromammal stable isotope data act as a proxy for local conditions, while macromammal data integrate information at a broader scale. Comparison of the stable carbon isotope data obtained from the micromammal and macromammal fossil specimens suggests that these two assemblage components intersected vegetation with differing proportions of C₄ grasses. Micromammal δ¹³C proxy data indicates that, immediately local to the site, a C₃ dominated vegetation was present, while the large mammal δ¹³C proxy data shows evidence of a vegetation community with a greater C₄ grass component that likely occurred somewhat more distant from the site itself on the Palaeo-Agulhas Plain.

© 2020 Elsevier Ltd. All rights reserved.

1. Introduction

Quaternary paleoenvironments in Africa are often contextualized within a framework of glacial/interglacial variation, where aridity during glacial periods significantly impacts the biogeography and diversity of both flora and fauna (e.g. (Schreiner et al., 2013)). However, local proxy records and vegetation modeling

both suggest highly variable regional paleoenvironmental responses to changes in major abiotic factors across the continent (Blome et al., 2012; Cowling et al., 2008; Scholz et al., 2007). This is especially true in many parts of southern Africa where distinctive local climatic and environmental features likely had unique responses to changing global factors, because these features arise independently of the primary drivers of climate/environmental change in the rest of Africa (Barrable et al., 2002; Chase and Meadows, 2007; Muller and Tyson, 1988; Reason and Rouault, 2005; Stuu et al., 2004). Marine isotope stage 6 (MIS 6) is a long glacial phase, but to date there are few proxy records from this time in the Cape Floristic Region (Marean et al., 2014).

In order to address the gap in information on MIS 6 conditions

* Corresponding author. African Centre for Coastal Palaeoscience, Nelson Mandela University, Port Elizabeth, Eastern Cape, 6031, South Africa.

E-mail addresses: tmatthews.matthews@gmail.com (T. Matthews), curtis.marean@asu.edu (C.W. Marean).

for the southern Cape of South Africa, we present here tandem micromammal and macromammal stable carbon and oxygen isotope data for one of only two fossil-bearing localities on the south coast of South Africa that is well-dated to the Middle Pleistocene (Jacobs, 2010; Marean et al., 2014; Rector and Reed, 2010), the MIS 6-age fossil hyena den Pinnacle Point 30 (PP30). Tandem micromammal and large mammal isotope data complement each other for a number of behavioural and ecological reasons, and have the potential to provide a more complete picture of local and regional vegetation and moisture than either data set alone. Isotopic data from micromammals and large mammals represent the prey of very different accumulators - in the case of PP30, brown hyena (*Parahyena brunnea*) and owls (likely the spotted eagle owl, *Bubo africanus*) (Matthews et al., 2019). Owls and hyenas sample distinct faunal communities (large versus small mammals), have very different ranges, and create accumulations that differ significantly in taxonomic representation. The predation ranges of raptors such as owls are comparably small ($r \sim 3$ km, or ~ 28.27 km²) when compared to the ranges of large carnivores such as hyenas (Andrews, 1990; Matthews, 2004; Mills, 1990).

Furthermore, these herbivorous mammalian taxa have distinctive life histories and foraging ranges. Small fauna tend to have restricted birthing seasons and lifespans, and similarly restricted home ranges. Large herbivores, even those not part of migration ecosystems, tend to have significantly larger ranges and to grow and develop more slowly. Thus, micromammals and large mammals sample different components of both site-local and regional environments, and time intervals. In ecotones or other localities where habitat heterogeneity is likely to have been present, direct comparison of the micromammal and large mammal stable isotope data may provide a more comprehensive view of paleovegetation that reflects taxon-specific behavior, herbivore foraging ranges and predator ranges.

The isotopic character of an animal's preferred food is reflected in that animal's isotopic profile, and thus the habitat from which the predator selects prey items is reflected in the isotopic composition of the fossil assemblages. This is the foundation of studies that utilize faunal isotopes to infer paleoenvironment (Ecker et al., 2018; Lee-Thorp, 2002; Lee-Thorp and Talma, 2000). We argue that these differing prey communities of owls and hyenas also likely sample different parts of the ancient ecosystem, with differing stable isotopic characteristics, and thus by considering accumulations of both we significantly enrich our understanding of past environments during the poorly sampled MIS 6.

Stable carbon and oxygen isotope data obtained from fossil tooth enamel have long been applied as proxies for paleoenvironmental conditions. Most of these data are from large mammalian fauna. Sampling of very small mammalian fauna to produce stable isotope data sets that reflect environmental conditions over a narrower geographic range is a relatively recent phenomenon (Gehler et al., 2012; Hopley et al., 2006; Hynes et al., 2012; Jeffrey et al., 2015; Thackeray et al., 2008; Yeakel et al., 2007a). This research has been driven in part by the realization that micromammal isotope data can provide statistically robust datasets and that small body size is less of a constraint for $\delta^{18}\text{O}$ than previously believed (Luz and Kolodny, 1985). Furthermore, methodological advances in mass spectrometry, such as laser ablation, now permit sampling of very small specimens (Cerling and Sharp, 1996; Lindars et al., 2001; Passey and Cerling, 2006; Richards et al., 2008; Sharp and Cerling, 1996).

2. Background

2.1. The site

PP30 (Fig. 1) is a paleontological locality that occurs within a

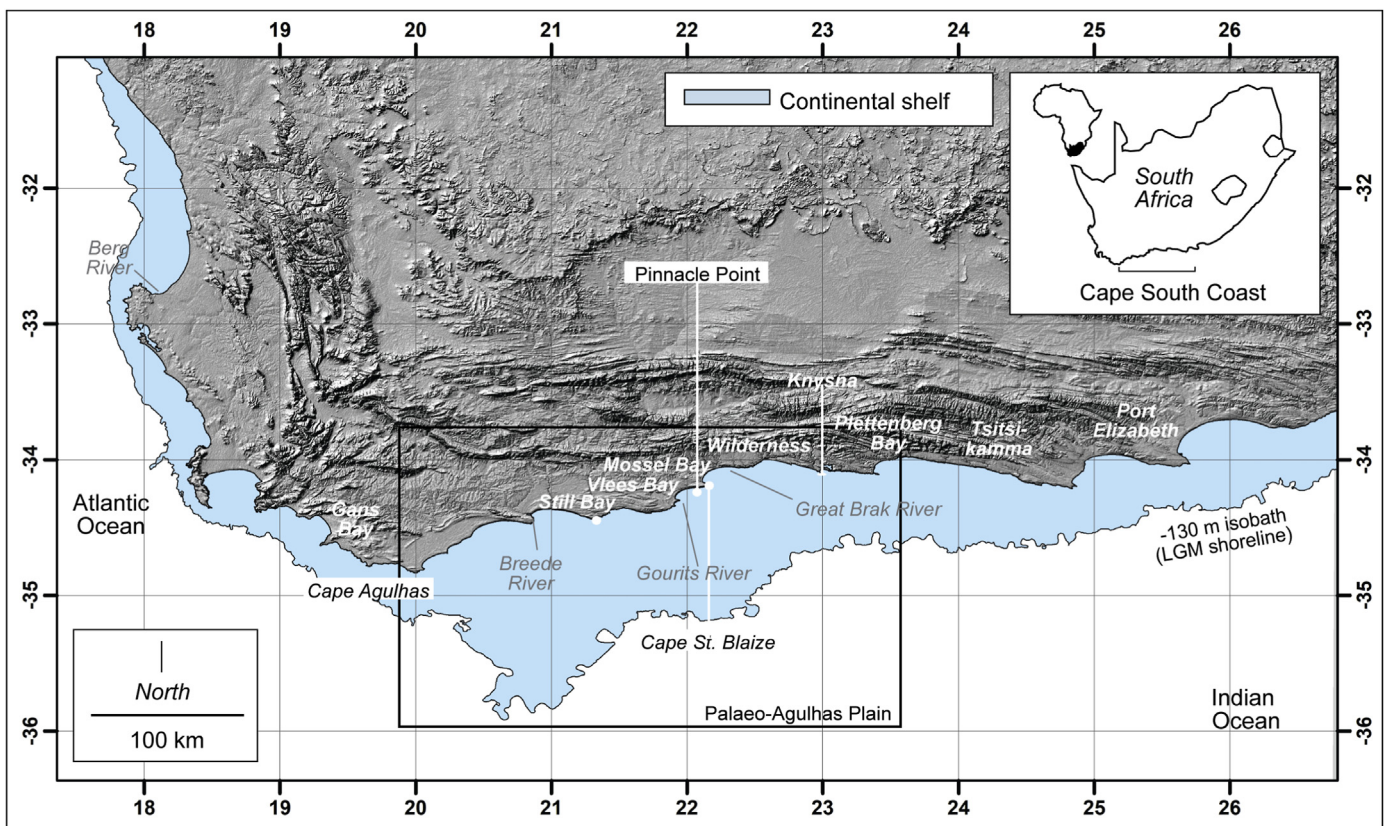


Fig. 1. The location of Pinnacle Point. Map courtesy of Hayley Cawthra, edited by Patrick Fahey.

cave in a calcrete layer stratified above the Table Mountain Sandstone cliffs at Pinnacle Point, South Africa (Rector and Reed, 2010). It was excavated as a salvage operation when it was discovered by trenching to lay pipes for a development. Excavations followed most of the procedures typical for excavations at Pinnacle Point (Bernatchez and Marean, 2011; Marean et al., 2004; Oestmo and Marean, 2014) though some strict requirements were relaxed due to the salvage nature of the excavations. All sediments were screened through nested 10 mm, 3 mm, and 1.5 mm screens, and additional fossil material was thus recovered. Optically stimulated luminescence (OSL) ages from sediment matrix indicate a relatively constricted period of deposition that dates to ~151 ka during the MIS 6 glacial. Paleoscape modeling of Pleistocene shorelines in the region (Fisher et al., 2010) puts the coast approximately 90 km from the site (Fig. 1). As such, during the accumulation phase it was at the ecotone between the Palaeo-Agulhas Plain (PAP) and the Cape coastal lowlands (CCL).

The large mammal faunal fossil assemblage from PP30 is previously published and contains ungulate taxa indicative of both grassland ecosystems and Cape flora (Marean et al., 2014; Rector and Reed, 2010). The abundance of carnivore-modified bone, hyena coprolites, and the lack of stone artifacts and cut-marked bone, implicates carnivores as the agent of accumulation of the faunal material. The abundance of fragmented ostrich eggshell and the presence of dental fragments attributable to *Parahyaena brunnea* (Rector and Reed, 2010), which are morphologically distinct from other hyenas, (Ewer, 1973), implicates brown hyena as the primary accumulator. Brown hyenas provision their young (Mills, 1990; Skinner et al., 1998; Skinner and Van Aarde, 1991), often bringing back complete or nearly complete carcasses as well as ostrich eggs, thus accounting for the composition of the PP30 assemblage. Most large mammals in the brown hyena diet are scavenged, and Mills (1990) observed that 66% of encountered carcass parts that were considered by him “suitable” for provisioning (still had nutrients) were carried back to the den for provisioning. For this reason, brown hyena dens accumulate bones rapidly. This, along with the minimal stratigraphic variation observed during excavation, and the uniformity of staining and fossilization of the fauna, suggests that the assemblage was accumulated over a comparably short period of geologic time (Rector and Reed, 2010), though we recognize that this is untestable with current dating methods due to the imprecision of those methods.

Mills observed that the average distance that provisioned items were carried was 6.4 km for brown hyenas, with some large items (sections of large antelope) being carried much further. Strontium isotope analysis of the grazing fauna (Copeland et al., 2016) and the ostrich eggshell (Hodgkins et al., 2018) collected by the brown hyenas from the site indicate the hyenas foraged primarily on the exposed Palaeo-Agulhas Plain, and thus the large mammal sample at PP30 captures a fairly large region to the south of the site on the plain.

The degree and type of digestive etching on the PP30 micro-mammal incisors is most similar to the pattern observed in spotted eagle owl (*Bubo africanus*) assemblages, and thus *Bubo africanus* is considered to be the aggregator of the small mammal portion of the assemblage, although the high frequency of un-etched incisors (~23% of the assemblage) is uncommon in modern eagle owl collections (Andrews, 1990; Matthews, n.d.).

The PP30 murid population is dominated by Otomyine species, including *Otomys unisulcatus*, cf. *O. sloggetti*, *O. angoniensis*, *O. karoensis*, and *O. irroratus*, and PP30 was the Pinnacle Point site which contained the greatest number of Otomyine species (Matthews et al., 2019). The latter two species dominate the assemblage at 29% and 43%, respectively, with the next most common rodent being *Rhabdomys pumilio* (10%). The other murid

taxa occurring at the site (*Myomyscus verreauxi*, *Gerbilliscus afra*, and *Zelotomys* cf. *woosnami*), and the two soricid species (*Myosorex varius* and *Suncus varilla*), occur in low frequencies of ~1–3%. There was clearly a selection for *Otomys* species by the owl that accumulated the PP30 micromammal assemblage, and the percentage occurrence of species suggests that the accumulation represents a relatively brief time. Using the PP30 micromammals for environmental interpretation is complicated by the fact that the assemblage shows low taxonomic diversity, is biased towards otomyines, and in addition, most of the species are environmentally adiagnostic as they are found in a diversity of habitats which generally include both fynbos/thicket and grassland habitats, and could reflect the presence of either, or both, of these vegetation types. The presence of *O. unisulcatus*, and *Gerbilliscus afra* suggests a dry, sandy component to the environment, whereas the presence of *O. irroratus* and *O. angoniensis* may indicate a wet facies or water source, such as a vlei or stream, in the area. The significance of *Zelotomys* cf. *woosnami* is discussed elsewhere (Matthews et al., 2019). However, the relatively low species diversity and the species' catholic dietary habits are advantageous factors when used for isotopic determinations of vegetation distributions in the past, as outlined below.

2.2. Environmental and climatic background

Most of southern Africa, with the exception of the westerly regions, falls under the influence of a summer rainfall regime that ultimately derives from the southward movement of warm wet airflow over the southern African interior (Tyson, 1999). Moisture is brought from the Indian ocean by the low-latitude Easterlies (or trade winds). Conversely, the southwest tip of Africa falls under the influence of moisture-bearing mid-latitude Westerlies that penetrate the southwestern corner of the sub-continent during the austral winter when the South Atlantic high pressure cyclonic system moves northwards. Winter rainfall also contributes to precipitation in the zone of year-round rain where the winter and summer rainfall regimes intersect to produce rainfall that shows less marked seasonality (Tyson, 1999). The Pinnacle Point locality currently falls within the year-round rainfall zone.

In present-day southern African plant communities there is a strong relationship between the predominant photosynthetic pathway of grasses and the occurrence of winter or bi-model/summer rain (Vogel et al., 1978). Grasses using C_4 photosynthesis dominate in most of the summer rainfall zone because they require warm growing season temperatures, while C_3 grasses are confined to those areas with cool growing seasons – in the winter-rainfall western zones and high altitude montane regions of the Drakensberg. In the GCFR the predominantly winter rainfall regime is dominated by shrubs and grasses that use the C_3 photosynthetic pathways, while C_4 grasses are significantly more common in those areas where rain falls in the summer (Cowling and Richardson, 1995; Cowling, 1983).

In terms of isotope ecology of the environment and climate, C_3 and C_4 photosynthetic pathways fractionate carbon isotopes (as part of CO_2 fixation) such that the tissues of C_4 plants are significantly enriched in $\delta^{13}C$ relative to C_3 plants (Smith and Epstein, 1971). Change in the relative contribution of C_4 grasses to paleovegetation communities in a region will be reflected in the isotopic composition of consumer diets and thus by extension consumer tissues, such that taxa with diets with a significant C_4 grass component will have comparably enriched $\delta^{13}C_{enamel}$ values relative to taxa consuming primarily C_3 -vegetation (Cerling and Harris, 1999; DeNiro and Epstein, 1978; Thorp and Van Der Merwe, 1987).

A number of factors contribute to the oxygen isotope composition of mammalian enamel in addition to the isotopic composition

of meteoric water. They include the oxygen isotopic composition of leafwater and plant carbohydrates that are influenced by evaporative enrichment under arid conditions, small-scale variability in the oxygen isotopic composition of different plant parts, and above all, whether an animal relies more heavily on environmental or plant water (Kohn et al., 1996; Sponheimer and Lee-Thorp, 1999). Since we lack controlled studies for the taxa sampled here, interspecific variation can partially be controlled for by analyzing data by taxon rather than aggregating it.

3. Methods

3.1. Materials: micromammals

A large sample of both cranial and post-cranial micromammal remains were recovered from PP30, both *in situ* and thus plotted by total station (electronic survey instrument), and in the screened sediments. Identification of murid taxa was made using the M¹ and M₁ teeth (*in situ* and isolated teeth) with the exception of the Otomyinae where the more diagnostic M³ was used, rather than the M¹. Soricids were quantified by mandibles and maxillae rather than single teeth as loose teeth were generally not recovered and these taxa were thus more accurately represented by mandibles and maxillae. The methodologies used to record the taphonomy of the assemblage are well established and described elsewhere (Fernandez-Jalvo and Andrews, 1992; Matthews et al., 2009, 2011). A full species list, and discussion of micromammal taxonomy at the site, is available (Matthews et al., 2019). As mentioned previously, the assemblage is dominated by the Otomyinae (vlei rats), and shows a low taxonomic diversity. The majority of micromammal species present in the assemblage occupy a broad diversity of habitats and thus are not diagnostic of any particular paleoenvironmental condition(s). Sampling of the micromammals for isotope analysis targeted particular taxa whose modern representatives are either herbivorous or (rarely) granivorous.

One-hundred and three micromammal teeth, including those with non-specific taxonomic identifications, were preliminarily identified in the field as suitable for analysis. Of these,

approximately half were exported for analysis per the heritage permit. Soricidae (*M. varius*) and Chiroptera (*Rhinolophus*) from the PP30 assemblage were not sampled because both taxonomic groups are insectivorous and thus their isotopic character may not reflect the vegetation in which they lived. *Mystromys albicaudatus* and *R. pumilio* specimens were also excluded due to omnivorous diets. One gerbillid (*G. afra*) specimen was sampled. An incisor specimen identified only as “indeterminate murid” was also analysed. The resulting taxonomic composition of the micromammal isotope sample is thus primarily composed of *Otomys* specimens. However, the relative representation of species in the isotope sample is similar to that in the larger assemblage, and thus we argue that it adequately represents the large/entire assemblage. Table 1 lists the PP30 micromammal sample.

Isolated teeth (and especially molars) are comparably more abundant in the PP30 assemblage than teeth that are *in situ* in the dental arcade. This is advantageous for laser ablation, as it reduces the frequency with which bony elements (such as mandibles and maxillae) need be placed in the vacuum chamber. Bone is significantly more porous than enamel and dentine, and thus can act as a reservoir of out-gassing interfering background CO₂ in the vacuum chamber after the chamber has been flushed with He gas. Exported specimens *in situ* in larger pieces of bone were not sampled; 2 specimens in which an incisor was present in a smaller fragment of the dental arcade were however ablated. *Otomys* molars are laminar, with complex surfaces on the buccal and lingual surfaces of the dentition, and variable dentine-enamel patterning on worn occlusal surfaces; Otomyine molars that are not *in situ* in the dental arcade present a comparably flat mesial surface suitable for ablation, as they can be arranged orthogonally to the direction of the laser.

3.2. Sampling procedures: micromammals

LA-GC-IRMS was performed at the stable isotope lab at Johns Hopkins University (Baltimore, USA), using published procedures (Passey and Cerling, 2006). Clean, dry teeth were mounted on an adjustable stand within a vacuum chamber, which was then

Table 1

PP30 sample. Tooth type sampled (by SACP4 specimen number). MU1 = 1st maxillary molar. MU3 = 3rd maxillary molar. ML1 = 1st mandibular molar.

Specimen Number	Taxon	Tooth Sampled	Number of Ablations	Plotted or Screened?
100464	Indet. mole rat	incisor	2	Screen
100475	Indet. mole rat	incisor	2	Screen
100491	Indet. mole rat	incisor	2	Screen
100486	Indeterminate murid	incisor	2	Plotted
100584b	<i>O. karoensis?</i>	incisor	2	Plotted
100584a	<i>O. karoensis</i>	MU3	1	Screen
100583	<i>O. karoensis</i>	MU3	1	Screen
100523	<i>O. karoensis</i>	MU3	2	Screen
100549	<i>O. karoensis</i>	ML1	1	Screen
100559	<i>O. karoensis</i>	ML1	1	Screen
100570	<i>O. karoensis</i>	ML1	1	Screen
100573	<i>O. karoensis</i>	ML1	1	Screen
100575	<i>O. karoensis</i>	ML1	1	Screen
100586	<i>O. karoensis</i>	ML1	2	Screen
100503	<i>O. irroratus</i>	MU3	1	Screen
100518	<i>O. irroratus</i>	MU3	1	Screen
100574	<i>O. irroratus</i>	MU3	1	Screen
100580	<i>O. irroratus</i>	MU3	2	Screen
100521b	<i>O. irroratus</i>	MU3	1	Screen
100505	<i>O. irroratus</i>	ML1	1	Screen
100511	<i>O. irroratus</i>	ML1	1	Screen
100522	<i>O. irroratus</i>	ML1	1	Screen
100589a	<i>O. irroratus</i>	ML1	1	Screen
100589b	<i>O. irroratus</i>	ML1	2	Screen
100534a	<i>G. afra</i>	MU1	1	Screen

flushed for a minimum of 4 h with inert He gas to remove the atmospheric CO₂ from the chamber. Blank measurements were taken at the beginning of each chamber run prior to ablation sampling to ensure that the He flush of the chamber was complete. Blank measurements were also taken at periodic intervals during each sampling run to ensure the integrity of the vacuum chamber (e.g. no leaks that might allow contaminant atmospheric CO₂ into the chamber), to monitor potential CO₂ off-gassing from specimens during the course of the sampling run, and to calculate background CO₂ blank fraction CO₂ peaks produced by specimen ablation.

Groups of specimen ablations were bracketed with measurement of a reference gas of known isotopic composition which was injected into the chamber both up- and down-stream of the samples. Isotope data obtained from fossil specimens was normalized to VPDB ($\delta^{13}\text{C}$) and VSMOW ($\delta^{18}\text{O}$), using the reference CO₂ values. Laboratory enamel standards were included in the sample chambers.

Each specimen was ablated using a Photon-Machines Fusions 30 W CO₂ laser operating at 5% power and with a dwell time of 0.01 s. Ablation produces CO₂ which is then transported by carrier He, and the gas sample(s) are aggregated and then cryofocused in a cold finger apparatus (Cerling and Sharp, 1996; Passey and Cerling, 2006; Sharp and Cerling, 1996). The He carrier gas is then separated from the CO₂ gas in the gas chromatograph and the CO₂ introduced into the mass spectrometer.

Ablation pit sizes were 30 μm in diameter, and between 10 and 40 ablation pits were produced for each specimen-sampling event. The production of multiple ablation pits for each enamel sample is required as single ablation events do not individually produce enough CO₂ gas for analysis by the IRMS. Each ablation pit sampled enamel adjacent to, but not overlapping, previous ablation pits (Fig. 2). The number of laser shots was increased when the area of blanks were slightly larger than ideal, in order to minimize the impact of residual CO₂ on the analytical signal produced by specimen ablation. The specimen stand within each chamber was adjusted between sampling of each specimen in order to rotate the surface of each tooth orthogonal to the path of the laser. Any ‘charring’ produced during the formation of an ablation pit is indicative of laser combustion of non-enamel organic material: six

ablation runs from five specimens were eliminated from the final analysis because significant ‘charring’ on the edge of the ablation pits was noted during the analysis.

3.3. Sampling procedures: large mammals

A suite of representative large herbivore teeth from the PP30 assemblage was selected for isotopic analysis (Table 2). Each tooth was first cleaned mechanically using a soft brush, and then the enamel surface abraded using a small rotary drill equipped with a burr at a low speed to remove any adhering matrix and the outermost enamel surface. Bulk enamel samples were taken by collecting approximately 5 mg of enamel powder using a diamond-

Table 2

The PP30 large mammal sample. Since there are no major changes observed in the stratigraphy at PP30, we have not indicated stratigraphic divisions or ages for each sample, and take them to be all roughly contemporary. ‘HAC’ = acetic acid pretreatment.

Sample ID	Scientific Name	Common Name	Treatment
66213	<i>Pelea capreolus</i>	Grey Rhebok	Not Acid Treated
115400	<i>Raphicerus melanotis</i>	Grysbok	Not Acid Treated
66552	<i>Raphicerus melanotis</i>	Grysbok	Not Acid Treated
66964	<i>Raphicerus melanotis</i>	Grysbok	Not Acid Treated
67181	<i>Raphicerus melanotis</i>	Grysbok	Not Acid Treated
115209	<i>Alcelaphus buselaphus</i>	Hartebeest	HAC
66613	<i>Alcelaphus buselaphus</i>	Hartebeest	HAC
66615	<i>Alcelaphus buselaphus</i>	Hartebeest	HAC
66751	<i>Alcelaphus buselaphus</i>	Hartebeest	HAC
66805	<i>Alcelaphus buselaphus</i>	Hartebeest	HAC
66997	<i>Alcelaphus buselaphus</i>	Hartebeest	HAC
67502–1	<i>Alcelaphus buselaphus</i>	Hartebeest	HAC
67502–2	<i>Alcelaphus buselaphus</i>	Hartebeest	HAC
67798	<i>Alcelaphus buselaphus</i>	Hartebeest	HAC
115250	<i>Antidorcas marsupialis</i>	Springbok	HAC
115358	<i>Antidorcas marsupialis</i>	Springbok	HAC
115374	<i>Antidorcas marsupialis</i>	Springbok	HAC
115426	<i>Antidorcas marsupialis</i>	Springbok	HAC
66769	<i>Antidorcas marsupialis</i>	Springbok	HAC
67129	<i>Antidorcas marsupialis</i>	Springbok	HAC
115248	<i>Connochaetes gnou</i>	Black Wildebeest	HAC
115433	<i>Connochaetes gnou</i>	Black Wildebeest	HAC
65534	<i>Connochaetes gnou</i>	Black Wildebeest	HAC
66586	<i>Connochaetes gnou</i>	Black Wildebeest	HAC
67367	<i>Connochaetes gnou</i>	Black Wildebeest	HAC
66316–11	<i>Hippotragus leucophaeus</i>	Blue Antelope	Not Acid Treated
115408	<i>Hippotragus leucophaeus</i>	Blue Antelope	Not Acid Treated
67836	<i>Hippotragus leucophaeus</i>	Blue Antelope	Not Acid Treated
67895	<i>Hippotragus leucophaeus</i>	Blue Antelope	Not Acid Treated
115208	<i>Damaliscus pygargus</i>	Bontebok	Not Acid Treated
115237	<i>Damaliscus pygargus</i>	Bontebok	Not Acid Treated
115349	<i>Damaliscus pygargus</i>	Bontebok	Not Acid Treated
115402	<i>Damaliscus pygargus</i>	Bontebok	Not Acid Treated
115411	<i>Damaliscus pygargus</i>	Bontebok	Not Acid Treated
67024	<i>Damaliscus pygargus</i>	Bontebok	Not Acid Treated
67149	<i>Damaliscus pygargus</i>	Bontebok	Not Acid Treated
115391	<i>Redunca arundinum</i>	Southern Reedbuck	Not Acid Treated
115327	<i>Redunca arundinum</i>	Southern Reedbuck	Not Acid Treated
66379	<i>Redunca arundinum</i>	Southern Reedbuck	Not Acid Treated
66899	<i>Redunca arundinum</i>	Southern Reedbuck	Not Acid Treated
66902	<i>Redunca arundinum</i>	Southern Reedbuck	Not Acid Treated
67278	<i>Redunca arundinum</i>	Southern Reedbuck	Not Acid Treated
67035	<i>Redunca arundinum</i>	Southern Reedbuck	Not Acid Treated
67532	<i>Redunca arundinum</i>	Southern Reedbuck	Not Acid Treated
67535	<i>Redunca arundinum</i>	Southern Reedbuck	Not Acid Treated
66967	<i>Redunca arundinum</i>	Southern Reedbuck	Not Acid Treated
67253	<i>Redunca arundinum</i>	Southern Reedbuck	Not Acid Treated
67661	<i>Redunca arundinum</i>	Southern Reedbuck	Not Acid Treated
115240	<i>Redunca arundinum</i>	Southern Reedbuck	Not Acid Treated
115363	<i>Redunca arundinum</i>	Southern Reedbuck	Not Acid Treated
66306	<i>Parahyaena brunnea</i>	Brown hyena	Not Acid Treated
115431	<i>Parahyaena brunnea</i>	Brown hyena	Not Acid Treated
115228	<i>Parahyaena brunnea</i>	Brown hyena	Not Acid Treated

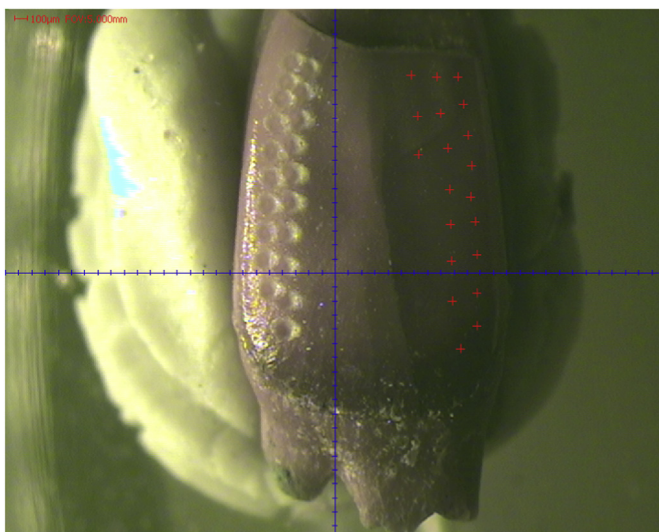


Fig. 2. Image of a mounted specimen after LA-GC-IRMS sampling. Ablation pits are visible along the left margin of the tooth surface. Note lack of char on pit margins and the non-overlapping nature of the ablation pits. The specimen is *O. saundersiae* from the Lower Roof Spall layer at PP13B (Specimen ID 99239, see ((Williams, 2015)).

tipped drillbit along the entire longitudinal axis of the tooth, avoiding cracks that could potentially introduce extraneous compounds.

The samples were analysed in two batches. The first followed a routine procedure (eg. (Lee-Thorp et al., 1997; Sponheimer and Lee-Thorp, 2001) in which the powders were reacted for 30 min in 1.5% (v/v) sodium hypochlorite solution, rinsed in Milli-Q distilled water, and leached in a weak acid solution (0.1 M acetic acid) for 10 min. This last step removes highly soluble carbonates if present but results in loss of bioapatite powder (ca. 40%). Treatment of the second batch of powders differed, as shown in Table 2; pretreatment was limited to washing in distilled water, following a series of experiments in our laboratory that suggest that, in addition to dissolving significant amounts of enamel powder, the above procedure is unnecessary in the case of unaltered, clean enamel and has minimal influence (<analytical uncertainty) on the isotope values (Jeffrey, 2016).

All samples were freeze-dried overnight, and 1.5–2 mg weighed into individual reaction vessels. CO₂ was produced by 100% H₃PO₄ acid hydrolysis at 72 °C in a Gasbench II, and introduced via a continuous-flow Gas Chromatograph (GC) for measurement in a Thermo Finnigan Delta V, in the University of Bradford Stable Light Isotopes Facility. Precision as estimated from standard deviations of multiple measurements of NBS 19 and the CarraraZ inter-laboratory standards was 0.1‰ for δ¹³C/δ¹²C, and 0.2‰ for δ¹⁸O/δ¹⁶O, while precision of two fossil enamel laboratory standards indicated precision of better than 0.1‰ for δ¹³C/δ¹²C, and 0.3‰ for δ¹⁸O/δ¹⁶O.

4. Results

4.1. Micromammals

Twenty-seven isolated and *in situ* micromammal teeth were sampled using LA-GC-IRMS. Data from five specimens were excluded due to char on the edges of the ablation pits and two others on the basis of large blank fractions, which potentially compromised the accuracy of isotope measurements. The remaining dataset is comprised of 28 isotope measurements made on 21

individual specimens.

Replicate measures were made on all 5 incisors sampled (2 sets of incisor replicate data excluded for char), as well as three of the Otomyine molar specimens, so as to check for consistency. Replicate isotope measurements are all concordant, with the difference between all replicate measurements well within 1‰ for both carbon or oxygen isotope values (δ¹³C mean σ = 0.31, δ¹⁸O mean σ = 0.27). Replicate LA-GC-IRMS measurements on molar and incisor teeth show similar precisions (Table 4) (δ¹³C_{incisor} mean σ = 0.27, δ¹⁸O_{incisor} mean σ = 0.26; δ¹³C_{molar} mean σ = 0.35, δ¹⁸O_{molar} mean σ = 0.27). This level of precision is lower than that obtained for conventional H₃PO₄ acid-digestion mass spectrometry, but is customary for LA-GC-IRMS and in accordance with measurement precision for the standards.

Two sets of replicate LA-GC-IRMS measurements of internal large mammal enamel standards were made during the collection of the PP30 micromammal isotope data (Table 3). The dispersion of LA-GC-IRMS carbon and oxygen data obtained from K00-TSV-223-1 and K00-AB-301-1 during the PP30 data collection period is larger than that of the replicate measurements made on the fossils themselves, but is within a range of acceptable precision for carbon and oxygen isotope measurements made on carbonates by Laser Ablation. The δ¹³C and δ¹⁸O values of K00-AB-301 and K00-TSV-223-1 are consistent with other LA-GC-IRMS-obtained values over a longer period (Williams, 2015). One (unavoidable) problem with solid enamel standards is that it is not isotopically homogenous through the crown. We thus suggest that their larger variation is largely attributable to sample heterogeneity (see Sharp and Cerling, 1996).

The δ¹³C_{enamel} VPDB values obtained by laser ablation of the fossil micromammal specimens range from −7.8‰ to −17.5‰, and are summarized by taxon in Table 4. We do not assume a normal distribution of the stable carbon isotopic composition of a population of animals from a given taxonomic group (as dietary variability is the driving factor in an individual's enamel isotope ratio); as such, comparisons of the isotopic composition of different populations from different taxonomic groups uses the non-parametric Kruskal-Wallis (KW) Test with Dunn's multiple comparison (post hoc) to test for significant differences in stable carbon

Table 3
Replicate values for fossil specimens from PP30.

Specimen ID	Taxon	Tooth	δ ¹³ C‰	diff δ ¹³ C‰	mean	stdev	δ ¹⁸ O _{SMOW} ‰	diff δ ¹⁸ O _{SMOW} ‰	mean	stdev
100464	Indet. mole rat	incisor	−11.8				25.1			
100464	Indet. mole rat	incisor	−12.4	0.6	12.11	0.43	25.2	0.1	25.15	0.05
100475	Indet. mole rat	incisor	−9.3				23.8			
100475	Indet. mole rat	incisor	−9.7	0.4	−9.52	0.31	24.3	0.5	24.01	0.34
100486	Indet. murid	incisor	−8.1				28.8			
100486	Indet. murid	incisor	−8	0.1	−8.09	0.07	28.2	0.5	28.49	0.38
100580	<i>O. irroratus</i>	MU3	−11.4				25.4			
100580	<i>O. irroratus</i>	MU3	−11.2	0.2	11.32	0.15	25.4	0	25.37	0.02
100523	<i>O. karoensis</i>	MU3	−17.5				22.8			
100523	<i>O. karoensis</i>	MU3	−17.1	0.4	17.28	0.28	23.2	0.5	23	0.34
100586	<i>O. karoensis</i>	ML1	−16.4				20.1			
100586	<i>O. karoensis</i>	ML1	−17.3	0.9	16.85	0.63	19.4	0.7	19.73	0.46

Table 4
Summary statistics for the stable carbon isotope data obtained from the PP30 micromammal specimens, by taxon.

	n	Minimum δ ¹³ C VPDB	Maximum δ ¹³ C VPDB	Mean δ ¹³ C VPDB	σ	range
<i>G. afra</i>	1	−13.9	−13.9	−13.9	–	–
Indet. mole rat	5	−12.4	−7.8	−10.2	1.885	4.6
Indet. murid	2	−8.1	−8	−8.1	0.071	0.1
<i>O. irroratus</i>	9	−16.1	−10.7	−13	1.931	5.4
<i>O. karoensis</i>	11	−17.5	−9.6	−14.1	2.643	7.9

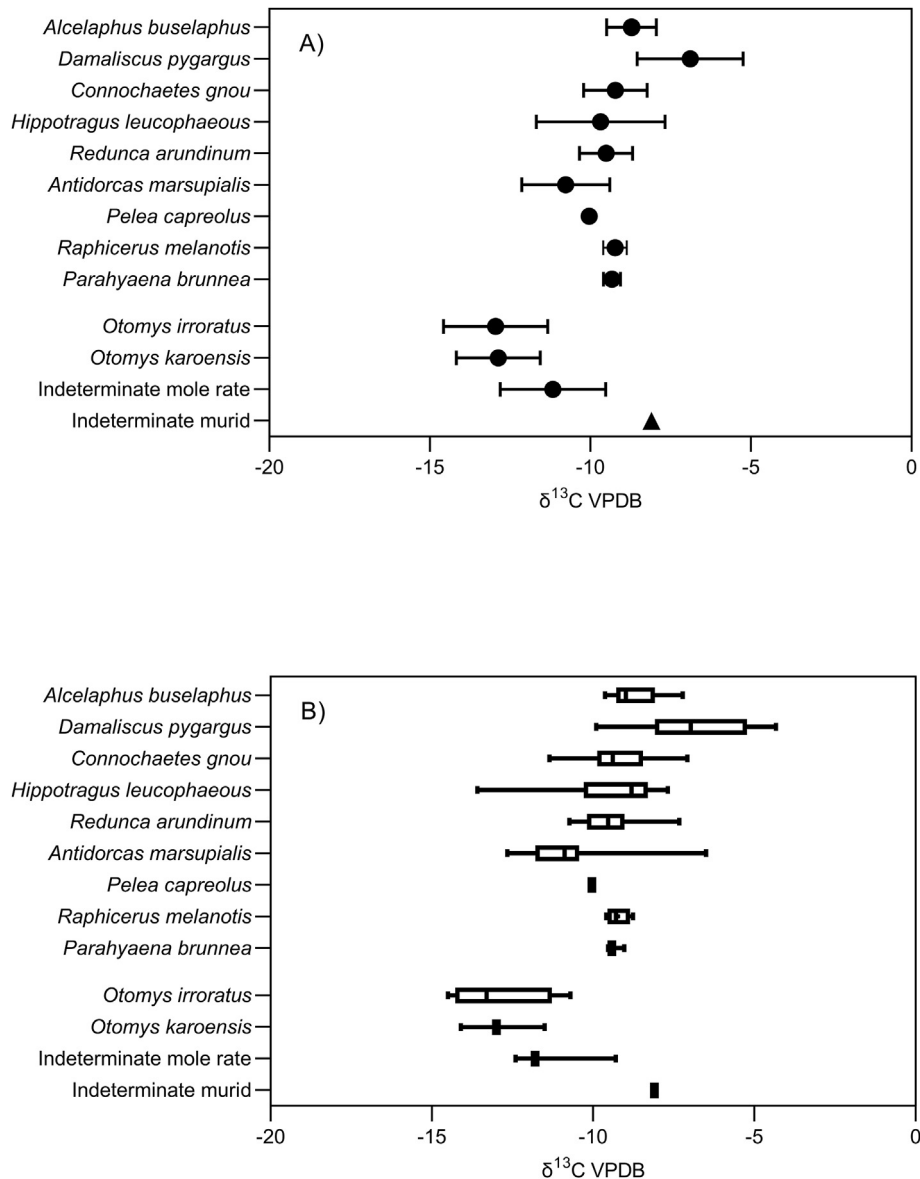


Fig. 3. Summary of the $\delta^{13}\text{C}$ values for the macromammals and micromammals. A) The mean and standard deviation, and B) the minimum and maximum with the mean plotted as a bar.

isotope composition between the *Otomys irroratus*, *Otomys karoensis*, and mole rat fossil populations reported here. *Gerbilliscus afra* and the indeterminate murid specimens were excluded from the KW Test because both samples have an n of 1. It should be noted however, that the indeterminate murid specimen (n = 1, sampled twice) appears to be considerably more enriched in ^{13}C than the other taxa in the PP30 sample ($\delta^{13}\text{C} = -8.1\text{‰}$ $\sigma = 0.07$, Fig. 3).

A KW test indicates significant differences between the stable carbon isotope values of the populations of *O. irroratus*, *O. karoensis*, and mole rats sampled ($H = 7.779$, $p = 0.0205$). Dunn's multiple comparison test ($\alpha = 0.05$) indicates the significant difference is only between the PP30 mole rats and the *O. karoensis* specimens. There is no significant difference between the stable carbon isotope composition of *O. irroratus* and *O. karoensis* populations, or *O. irroratus* and the mole rats. Furthermore, there is a large (but non-significant) difference between the mean $\delta^{13}\text{C}$ values of the *O. irroratus* and the mole rat sample populations, and a very small

difference between the mean $\delta^{13}\text{C}$ values of the two *Otomys* species. This general pattern is consistent with analyses of other micromammal data from the region (Williams, 2015) in which the mole rats are comparably more enriched in ^{13}C than other micromammal taxa.

The stable carbon isotope values obtained from the micromammal specimens indicates that the taxonomic group labeled "mole rats" ($n_{\text{individuals}} = 3$, $n_{\text{samples}} = 5$) were likely mixed feeders, with modest but varying proportions of C_4 vegetation in their diets ($\delta^{13}\text{C}_{\text{enamel}} = -7.8\text{‰}$; $-12.1\text{‰} \pm 0.43$; $-9.5\text{‰} \pm 0.31$, see (Williams, 2015) for details on the calculations).

The Otomyiinae (*O. irroratus*, *O. karoensis*) span the spectrum from pure C_3 to mixed C_3/C_4 feeders. This wide range of $\delta^{13}\text{C}$ values for the Otomyiinae is consistent with what is known of their feeding ecology; *O. irroratus* will consume most vegetation in its habitat (Skinner and Chimimba, 2005), but it appears to be a preferential grazer when grasses are available (De Graaff, 1981; Skinner and

Chimimba, 2005). The diet of *O. karoensis* is less well-understood (Skinner and Chimimba, 2005), but given morphological similarities to other closely related species of *Otomys*, as well as the fact that it co-occurs with *O. irroratus* in all the Pinnacle Point fossil micromammal accumulations, it most likely shares similar diet breadth to other members of the genus. There are no pure C_4 feeders in the micromammal assemblage, as indicated by the $\delta^{13}C_{\text{enamel}}$ values of the specimens sampled here. Even the relatively ^{13}C -enriched murid specimen 100486 is a mixed C_3/C_4 feeder.

The interpretation of $\delta^{18}O_{\text{enamel}}$ data is complicated by a number of factors in addition to factors associated with precipitation. Offsets between laser and conventional measurements on fossil and modern enamel occur because a mixture of carbonate, phosphate and hydroxyl oxygen is ablated. Since the two main oxygen-bearing ions, PO_4 and CO_3 , differ strongly in abundance (the former dominates), and in isotope value (by approximately 9‰), this mixture produces values tilted towards PO_4 that are not directly comparable with the acid-digestion procedure and are more imprecise. Passey and Cerling (2006) observed a mean laser-conventional offset of $-6.4\text{‰} \pm 0.7$ in controlled experiments on fossil enamel. The systematic depletion in ^{18}O of the PP30 fossil micromammal specimens when compared to the large fauna (Fig. 4) is consistent with this. Nonetheless, large scale changes in oxygen isotope composition of enamel are resolvable (Passey and Cerling, 2006).

$\delta^{18}O_{\text{enamel}}$ VSMOW values for the PP30 micromammals range from 17.6‰ to 28.8‰. Comparison of the $\delta^{18}O_{\text{enamel}}$ values by taxon suggests that the lone specimen of *G. afra* ($\delta^{18}O_{\text{enamel}}$ VSMOW = 17.6‰; mean values of $\delta^{18}O_{\text{enamel}}$ VSMOW for *O. irroratus* = $22.4\text{‰} \pm 2.21$; for *O. karoensis* = $23.15\text{‰} \pm 2.32$; for mole rats = $24.42\text{‰} \pm 0.71$) appears to be low relative to the rest of the micromammal population (Fig. 4), while the single specimen of indeterminate murid is somewhat enriched ($\delta^{18}O_{\text{enamel}}$ VSMOW = $28.5\text{‰} \pm 0.42$). KW test of the *O. irroratus*, *O. karoensis*, and 'mole rat' populations show no significant difference in the oxygen isotope ratios of those populations of specimens ($H = 1.876$, $p = 0.3914$). These data suggest that while the difference in $\delta^{13}C_{\text{enamel}}$ values of the micromammal specimens are sampling real variability in the composition the plant remains consumed by the individual animals, the statistically similar $\delta^{18}O_{\text{enamel}}$ values of the mole rats and *Otomys* specimens suggest broad similarities in oxygen isotope ecology between these taxa.

4.2. Large mammals

Fifty-two taxonomically identified large mammal fossil teeth from PP30 were sampled for carbon and oxygen isotope analysis (one specimen, an Alcelaphine tooth #67502, was sampled twice, for a total sample $n = 53$). Taxa sampled for isotopic analysis represent browsing antelope species (*Pelea capreolus* and *Raphicerus melanotis*), mixed feeders who primarily consume browse but may include grass in their diets (*Antidorcas marsupialis*), and grazing taxa (*Alcelaphus buselaphus*, *Connochaetes gnou*, *Hippotragus leucophaeus*, *Damaliscus pygargus*, *Redunca arundinum*). Three brown hyena specimens (*Parahyaena brunnea*) were also analysed (Table 5).

The $\delta^{13}C_{\text{enamel}}$ VPDB values obtained from the PP30 large fauna specimens range from -9.9‰ to -5.6‰ . Mean $\delta^{13}C_{\text{enamel}}$ values of the browsing taxa (*P. capreolus*, *R. melanotis*) are depleted in ^{13}C by only $\sim 1\text{‰}$ relative to the other large herbivorous taxa from PP30 (browser $\delta^{13}C_{\text{enamel}} = -9.39$, $\sigma = 0.48$; mixed feeder $\delta^{13}C_{\text{enamel}} = -8.53\text{‰}$, $\sigma = 1.01$; grazer $\delta^{13}C_{\text{enamel}} = -8.23\text{‰}$, $\sigma = 0.96$). No significant differences in $\delta^{13}C$ are detected when specimens are grouped by taxon (KW test, $H = 11.60$, $p = 0.1146$). However, when samples are grouped by feeding behavior (browser, mixed feeder, or grazer), the populations of carbon isotope values are significantly different (although still small) between browsers and grazers (KW test, $H = 8.725$, $p = 0.0127$, Dunn's multiple comparison test). Isotopic variability within these feeding behavior categories also differs. Browser $\delta^{13}C_{\text{enamel}}$ values are relatively restricted, ranging from -10.0‰ to -8.8‰ , while mixed feeders and grazers exhibit a wider range: mixed feeders between -9.6‰ and -6.1‰ , and grazer values from -9.9‰ to -5.6‰ (Fig. 3). Thus, while there is significant overlap in the more negative $\delta^{13}C_{\text{enamel}}$ values obtained from all sampled taxa, some specimens of taxa that engage in either obligate or facultative grazing have higher $\delta^{13}C_{\text{enamel}}$ values relative to both PP30 browsing taxa and PP30 grazing conspecifics. Thus the higher $\delta^{13}C_{\text{enamel}}$ values reflect a larger C_4 grass component in the diets of some of the grazers, but not all of them.

Almost all of the PP30 fossil large herbivores sampled, regardless of inferred feeding behavior, have enamel values that are ^{13}C -enriched compared to those of modern or historical fauna. For instance, $\delta^{13}C_{\text{enamel}}$ values for each taxonomic group sampled in the

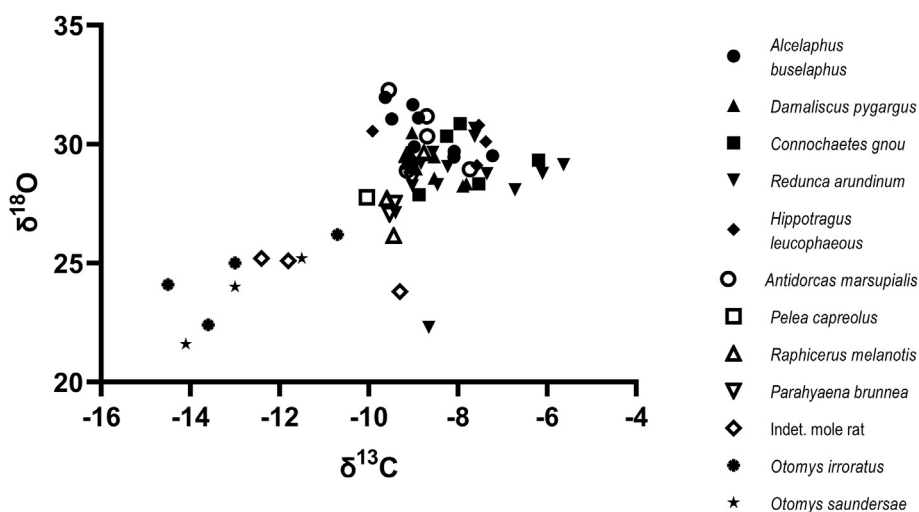


Fig. 4. Bivariate plot of $\delta^{13}C$ versus $\delta^{18}O$ for all the measured specimens. It must be noted that for the micromammals, $\delta^{18}O$ obtained by laser ablation is not directly comparable to values obtained by acid digestion because of the resulting mixture of oxygen from phosphate and carbonate in the former, as explained above.

Table 5
Isotopic data for the macromammals from PP30.

Sample ID	Scientific Name	$\delta^{13}\text{C}$	$\delta^{18}\text{O}$
66213	<i>Pelea capreolus</i>	-10.0	27.8
115400	<i>Raphicerus melanotis</i>	-9.6	27.7
66552	<i>Raphicerus melanotis</i>	-9.4	26.2
66964	<i>Raphicerus melanotis</i>	-9.1	29.6
67181	<i>Raphicerus melanotis</i>	-8.8	29.6
115209	<i>Alcelaphus buselaphus</i>	-8.9	31.1
66613	<i>Alcelaphus buselaphus</i>	-8.1	29.5
66615	<i>Alcelaphus buselaphus</i>	-9.0	31.7
66751	<i>Alcelaphus buselaphus</i>	-8.1	29.7
66805	<i>Alcelaphus buselaphus</i>	-9.1	29.4
66997	<i>Alcelaphus buselaphus</i>	-7.2	29.5
67502-1	<i>Alcelaphus buselaphus</i>	-9.6	32.0
67502-2	<i>Alcelaphus buselaphus</i>	-9.5	31.1
67798	<i>Alcelaphus buselaphus</i>	-9.0	29.9
115250	<i>Antidorcas marsupialis</i>	-9.1	29.2
115358	<i>Antidorcas marsupialis</i>	-9.6	32.3
115374	<i>Antidorcas marsupialis</i>	-9.1	28.9
115426	<i>Antidorcas marsupialis</i>	-8.7	31.2
66769	<i>Antidorcas marsupialis</i>	-7.7	29.0
67129	<i>Antidorcas marsupialis</i>	-8.7	30.3
115248	<i>Connochaetes gnou</i>	-8.9	27.9
115433	<i>Connochaetes gnou</i>	-7.5	28.3
65534	<i>Connochaetes gnou</i>	-6.2	29.3
66586	<i>Connochaetes gnou</i>	-7.9	30.9
67367	<i>Connochaetes gnou</i>	-8.3	30.3
66316-11	<i>Hippotragus leucophaeus</i>	-9.9	30.5
115408	<i>Hippotragus leucophaeus</i>	-7.6	29.1
67836	<i>Hippotragus leucophaeus</i>	-7.4	30.1
67895	<i>Hippotragus leucophaeus</i>	-7.5	30.8
115208	<i>Damaliscus pygargus</i>	-8.5	29.5
115237	<i>Damaliscus pygargus</i>	-7.9	28.2
115349	<i>Damaliscus pygargus</i>	-9.1	29.2
115402	<i>Damaliscus pygargus</i>	-9.0	30.5
115411	<i>Damaliscus pygargus</i>	-8.9	29.0
67024	<i>Damaliscus pygargus</i>	-8.5	28.6
67149	<i>Damaliscus pygargus</i>	-7.8	28.3
115391	<i>Redunca arundinum</i>	-9.0	29.0
115327	<i>Redunca arundinum</i>	-8.5	28.3
66379	<i>Redunca arundinum</i>	-8.7	22.3
66899	<i>Redunca arundinum</i>	-8.6	29.7
66902	<i>Redunca arundinum</i>	-6.7	28.1
67278	<i>Redunca arundinum</i>	-7.3	28.8
67035	<i>Redunca arundinum</i>	-5.6	29.1
67532	<i>Redunca arundinum</i>	-7.6	30.7
67535	<i>Redunca arundinum</i>	-8.2	29.1
66967	<i>Redunca arundinum</i>	-9.0	28.3
67253	<i>Redunca arundinum</i>	-6.1	28.8
67661	<i>Redunca arundinum</i>	-9.4	27.1
115240	<i>Redunca arundinum</i>	-7.6	30.3
115363	<i>Redunca arundinum</i>	-8.8	29.2
66306	<i>Parahyaena brunnea</i>	-9.0	28.5
115431	<i>Parahyaena brunnea</i>	-9.4	27.5
115228	<i>Parahyaena brunnea</i>	-9.5	27.1

PP30 fossil assemblage are more enriched in ^{13}C than other herbivorous taxa from C_3 vegetation communities in South Africa (Lee-Thorp et al., 1989; Sponheimer and Lee-Thorp, 2003; Thorp and Van Der Merwe, 1987) and in East Africa (Cerling and Harris, 1999). The lowest values from PP30 large faunal specimens barely overlap with $\delta^{13}\text{C}_{\text{enamel}}$ values (-14.9‰ to -9.3‰) reported from the clearly C_3 early Pliocene assemblage of Langebaanweg on the Western Cape, South Africa (Franz-Odenaal et al., 2002). A similar phenomenon has been noted for glacial period faunas in the South-western Cape and elsewhere (Hare and Sealy, 2013). It has been suggested that low pCO_2 during deep glacials resulted in more positive plant $\delta^{13}\text{C}$ values, which are passed onto the animals that feed on them (Hare et al., 2018). Given that the PP30 assemblage formed in a strong Glacial, we suggest that this is the most likely explanation for the relatively positive values for the fauna.

A number of taxa found in the PP30 assemblage are in the present day associated with specific habitat types. *R. melanotis*, a browser, is endemic to the GCFR, associated with fynbos vegetation, and prefers dense vegetation cover (Estes, 1991; Kingdon, 2015). The $\delta^{13}\text{C}_{\text{enamel}}$ values of fossil *R. melanotis* from PP30 ($= -9.11\%$, $\sigma = 0.35$, $n = 3$) are among the lower stable carbon isotope values from the PP30 large fauna but they are still more positive than expected for *R. melanotis* today (even when modern values are corrected for the fossil fuel effect). *A. buselaphus*, *A. marsupialis*, and *C. gnou* are in particular associated with open grassland ecosystems. Mean carbon isotope values for fossil exemplars from PP30 (Fig. 3), while slightly higher relative to *R. melanotis*, suggest only small C_4 grass contributions; thus grassy cover was dominated by C_3 varieties.

In fact, all fossil specimens of grazing taxa from PP30 have $\delta^{13}\text{C}_{\text{enamel}}$ values that are notably depleted when compared to $\delta^{13}\text{C}_{\text{enamel}}$ data reported from ecosystems dominated by C_4 grasses, such as in the north of South Africa (Sponheimer et al., 2003: Tabl 8). Taking the relatively high $\delta^{13}\text{C}_{\text{enamel}}$ values for known browsers such as *R. melanotis* into account, it seems that carbon isotope distribution for the entire ecosystem is shifted to relatively higher values (see discussion above). Therefore, while the PP30 known grazers are slightly ^{13}C -enriched compared to the known browsers, the results suggest very minor proportions of C_4 grasses in their diets. That in turn implies rather minor proportions of C_4 grass in the vegetation communities proximate to PP30 at ~151ka.

5. Discussion

Because the fossil assemblages from PP30 represent a fairly constrained period of deposition, the micromammal and large faunal material can be treated as contemporaneous and the isotope data as proxies of paleoenvironmental conditions near to the site at ~151 ka, a phase of MIS6 indicated by deep sea core and ice core records to be a strong phase of glacial cooling. However, taken separately, analyses of the PP30 fossil micromammal and the PP30 fossil large mammal carbon and oxygen isotope data, respectively, do not appear immediately concordant. Both the $\delta^{18}\text{O}$ and $\delta^{13}\text{C}$ values obtained from the micromammal fossils are considerably lower when compared to even the most depleted $\delta^{13}\text{C}$ values from the large fauna (Fig. 4).

The oxygen isotope difference between the means of these populations is 5.428 ± 0.5264 (95% CI = 4.359 to 6.498), is consistent with the offsets reported for specimens analysed using both LA-GC-IRMS vs H_3PO_4 acid hydrolysis methods (*laser-acid) of $-5.1\% \pm 1.2$ for fossil specimens (Passey and Cerling, 2006). The apparent distinction between the PP30 micromammal and the PP30 large fauna $\delta^{18}\text{O}$ values is thus an analytical artifact.

The generally more-depleted $\delta^{13}\text{C}_{\text{enamel}}$ values of the PP30 micromammals relative to the PP30 large fauna, however, are unlikely to be a result of the different analytical methods. The difference in this case is attributable to a reduced tissue-diet enrichment factor ($\epsilon_{\text{enamel-diet}}$) for rodents (Hynek et al., 2012); assuming a decrease in tissue-diet enrichment factor as large as 3‰ (an $\epsilon_{\text{enamel-diet}}$ of 11‰ for small mammals vs 14‰ for ungulates, see Cerling and Harris, 1999; Hynek et al., 2012; Passey et al., 2005; Podlesak et al., 2008), many PP30 micromammal stable carbon isotope values are still relatively depleted compared to the large mammal fauna. If we exclude methodological or analytical artifacts, the distinction rather reflects dietary differences in the relative proportions of C_3 and C_4 of these large and small primary consumers, and the closed or open nature of their preferred habitats during MIS6.

In addition to being comparably enriched in ^{13}C relative to the PP30 micromammals, the intraspecific range of stable carbon

isotope values are narrower in the large fauna. Given the catholic dietary preferences of many small mammals (Leichtler et al., 2016) the wide range of intraspecific $\delta^{13}\text{C}$ variation within the fossil *Otomyines* is suggestive of a local environment that, given the comparably depleted stable carbon isotope values of these taxa, is dominated by C_3 vegetation cover but with some component of C_4 grass in the nearby environment. The range of *O. karoensis* and *O. irroratus* $\delta^{13}\text{C}_{\text{enamel}}$ values (-17.5‰ to -9.6‰ , and -16.10‰ to -10.7‰) overlap with the large fauna stable carbon isotope data reported for the C_3 Pliocene Langebaanweg fossil assemblage (-14.9‰ to -9.3‰ , Franz-Odenaal et al., 2002) and for modern/historical large C_3 consumers in the Cape (approximately -16‰ to -13‰ , Lee-Thorp et al., 1989). The results are thus strongly suggestive of C_3 dominated vegetation in the immediate vicinity of PP30 at ~151yr.

Although the most depleted of mole rat $\delta^{13}\text{C}_{\text{enamel}}$ values overlap with the most enriched specimen of the *Otomyinae*, the distribution of carbon isotope ratios in the mole rats sampled are statistically distinct from those of the other small mammals. The mole rat $\delta^{13}\text{C}_{\text{enamel}}$ values overlap with the most depleted values found in the large fauna dataset, indicating a greater C_4 component of mole rat diets (when compared to *Otomyines*) during MIS 6. Modern mole rats primarily consume geophytic parts of plants, as well as grasses and sedges, although the taxonomic variability of the flora in the diet varies between species (Davies and Jarvis, 1986). Although there is limited data available, C_3 geophytes are not notably enriched relative to other C_3 plants, nor are C_4 geophytes depleted relative to C_4 grasses (Codron et al., 2005). Consumption of C_4 geophytes is therefore unlikely to be the dietary source of the enriched PP30 mole rat stable carbon isotope values observed; instead we argue that the modest enrichment of mole rat enamel is due to a dietary grass or sedge fraction. Specific identification of the mole rats sampled here was not possible on diagnostic grounds, however the stable carbon isotope values of the PP30 mole rats ($\delta^{13}\text{C}_{\text{enamel}} = -12.4$ to -7.8) are intermediate between values reported for modern *Georychus capensis* (approximately -16‰ to -11.5‰) and *Bathyergus suillus* (approx. -9‰ to -4‰) specimens from C_3 -dominated vegetation communities in the Western Cape (Yeakel et al., 2007b).

The stable carbon isotope composition of the most ^{13}C -depleted specimens of the *Otomys* sampled here reflect pure C_3 feeding behavior; the $\delta^{13}\text{C}_{\text{enamel}}$ values of these *Otomyine* specimens are considerably more depleted than the most depleted values of any large fossil fauna from PP30, including those that are, by modern analogy, browsing species (*P. capreolus* and *R. melanotis*). PP30 *P. capreolus* and *R. melanotis* values ($\delta^{13}\text{C}_{\text{enamel}}$ range from -10.0‰ to -8.8‰) are enriched in ^{13}C by about 3‰ when compared to the values reported for modern C_3 -consuming large fauna in the Cape (Lee-Thorp et al., 1989), and overlap only with the most enriched end-members of the range of $\delta^{13}\text{C}$ values for herbivorous fossils from Langebaanweg. All fossil grazers and mixed-feeding taxa from PP30 fall outside the range of carbon isotope values reported for modern Cape fauna (e.g. the PP30 fauna is more enriched in ^{13}C).

None of the large fossil specimens from PP30 have $\delta^{13}\text{C}_{\text{enamel}}$ values as positive as modern fauna that live in C_4 grassland ecosystems. This suggests that the large fauna from PP30, especially the obligate grazing species, consumed a range of paleovegetation with a significant C_3 grass component while concomitantly having C_4 grasses available for graze. Clearly, the macromammals, in particular the grazers, reflect a broader environment that reaches into regions which did have C_4 grasses, while the micromammals did not. Strontium isotope analyses of the large ungulate fauna from PP30 show that they lived nearly exclusively on the Palaeo-Agulhas Plain (Copeland et al., 2016), and it has been hypothesized that they were part of an east-west migration ecosystem

(Marean, 2010). Movement of this type where the ungulates would consume more C_4 grass in the summer-centered months while resident in the east, and more C_3 grass in the winter-centered months while in the west, might explain the mixed signal. A serial isotope analysis study presented in this volume (Hodgkins et al., 2020) shows that some specimens have modest to significant seasonal shifts in the dietary composition of C_3 and C_4 grass, and this is likely the reason the bulk sampled isotope values in this study show a greater enrichment of the $\delta^{13}\text{C}_{\text{enamel}}$ values relative to the micromammals.

The hunting range of the aggregating predator (*Bubo africanus* or other closely related owl species) of the micromammal component of the PP30 is comparably small ($r = 3$ km, or ~ 28.27 km² (Andrews, 1990; Matthews, 2004), and likely samples environments immediately proximate to the site itself. The $\delta^{13}\text{C}_{\text{enamel}}$ data obtained from the micromammal specimens at PP30 suggests the presence of C_3 -dominated vegetation, with only a small component of C_4 grasses. This is consistent with a number of GCFR vegetation community types extant in the region in the present day. The current vegetation surrounding the Pinnacle Point cliffs includes limestone fynbos on the cliffs where calcretes are present, and this is relatively extensive. This calcrete is ancient, probably Miocene, so was certainly present in MIS 6. This limestone fynbos is dominated by C_3 shrubs, with rarer grasses that can include both C_3 and C_4 types. On the slopes of the dunes that drape some of the lower portions of the cliffs is Strandveld vegetation, which is dominated by C_3 shrubs and trees. Stable carbon isotope data from mole rats is within the range of carbon isotope values obtained from modern model rat specimens from the Western Cape: combined with the strongly C_3 fossil *Otomys* carbon isotope signal, the fossil micromammal carbon isotope data does not suggest that this fynbos vegetation at PP30 was replaced during glacial MIS 6 by C_4 grasses.

The owls accumulating the micromammals at PP30 would have been sampling a habitat dominated by C_3 vegetation, while the brown hyenas accumulating the large fauna, with their greater foraging radius and preference for large bodied fauna, could have sampled a habitat with the potential for a much wider range of vegetation, including the Palaeo-Agulhas Plain. The range of the aggregating predator (*Parahaena brunnea*) of the large mammal faunal sample is considerably larger (>170 km², depending on habitat heterogeneity (Wiesel, 2006). Comparison of the fossil large mammal $\delta^{13}\text{C}_{\text{enamel}}$ data and the fossil micromammal $\delta^{13}\text{C}_{\text{enamel}}$ data from PP30 strongly suggests that these two assemblage components sampled different vegetation communities. The PP30 micromammal stable carbon isotope values are consistent with C_3 vegetation as common to this area today, while values for the PP30 large fauna indicate that some of the grazers had access to C_4 grass resources that are not reflected in the diets of the small fauna, and thus were not likely to occur in the area immediate (within ~3 km) of the site. The speleothem records (Braun et al., 2018, 2019) unfortunately have a gap surrounding 151 ka, but overall the preserved MIS 6 record in the speleothem shows a mixed C_3 - C_4 signal, and less C_4 than MIS 4.

6. Conclusions

The stable isotopes, $\delta^{13}\text{C}$ and $\delta^{18}\text{O}$, of micromammals and macromammals from an MIS 6 paleontological site at Pinnacle Point (PP30) were compared. The vast majority of micromammals were accumulated by owls, while the macromammals were accumulated by brown hyenas. The results are consistent with sampling of the paleovegetation at different geographic scales. Taking into account the differences occasioned by the analytical methods – LA-GC-IRMS and H_3PO_4 -IRMS – micromammal stable isotope data act as a proxy for local conditions, while macromammal data integrate

information at a broader scale. Comparison of the stable carbon isotope data obtained from the micromammal and macromammal fossil specimens suggests that these two assemblage components intersected vegetation with differing proportions of C_4 grasses. Micromammal $\delta^{13}C$ proxy data indicates that, immediately local to the site and at the ecotone between the Palaeo-Agulhas Plain and the Cape coastal lowland, a C_3 dominated vegetation was present, while the grazing large mammal $\delta^{13}C$ proxy data shows evidence of a vegetation community dominated by C_3 grass but with a greater C_4 grass component that likely occurred somewhat more distant from the site itself on the Palaeo-Agulhas Plain.

Acknowledgments

The authors would like to thank the MAPCRM crew for their invaluable assistance; B. Genari for laboratory and catalogue assistance at the Diaz Museum; A. Miller, A. Sommerville, and A. Michaud for advice and assistance with the sample preparation and data collection of the Wilderness modern micromammal data; K. Knudsen for laboratory space in the Archaeological Chemistry Laboratory (ASU). We also thank B. Passey for access to and training on the LA-GC-IRMS at Johns Hopkins University, and H.L. Williams for logistical support in Baltimore; and Andrew Gledhill in the Stable Light Isotopes Facility at the University of Bradford. This research was supported by the National Science Foundation grants to Marean (BCS-0524087 and BCS-1138073), the Late Lessons from Early History grant, the Hyde Family Foundation, a School of Human Evolution and Social Change Graduate Research award (to HM Williams), and a SHESC dissertation writing fellowship (to HM Williams), and the University of Bradford (to JA Lee-Thorp). Destructive analysis permits were granted by the South African Heritage Resource Agency. The support of the DST-NRF Centre of Excellence in Palaeosciences (COE-Pal) towards this research is hereby acknowledged. Financial support was also received from the National Research Foundation of South Africa. Judith Sealy and a referee provided helpful comments.

References

Andrews, P., 1990. *Owls, Caves, and Fossils: Predation, Preservation, and Accumulation of Small Mammal Bones in Caves, with an Analysis of the Pleistocene Cave Faunas from Westbury-Sub-Mendip, Somerset, UK*. University of Chicago Press, Chicago.

Barrable, A., Meadows, M.E., Hewitson, B.C., 2002. Environmental reconstruction and climate modelling of the Late Quaternary in the winter rainfall region of the Western Cape, South Africa. *South Afr. J. Sci.* 98, 611–616.

Bernatchez, J., Marean, C.W., 2011. Total station archaeology and the use of digital photography. *SAA Archaeol. Rec.* 11, 16–21.

Blome, M.W., Cohen, A.S., Tryon, C.A., Brooks, A.S., Russell, J., 2012. The environmental context for the origins of modern human diversity: a synthesis of regional variability in African climate 150,000–30,000 years ago. *J. Hum. Evol.* 62, 563–592. <https://doi.org/10.1016/j.jhevol.2012.01.011>.

Braun, K., Bar-Matthews, M., Matthews, A., Ayalon, A., Cowling, R.M., Karkanas, P., Fisher, E.C., Dyez, K., Zilberman, T., Marean, C.W., 2018. Late Pleistocene records of speleothem stable isotopic compositions from Pinnacle Point on the South African south coast. *Quat. Res.* 1–24. <https://doi.org/10.1017/qua.2018.61>.

Braun, K., Bar-Matthews, M., Matthews, A., Ayalon, A., Zilberman, T., Cowling, R.M., Fisher, E.C., Herries, A.I.R., Brink, J.S., Marean, C.W., 2019. Comparison of climate and environment on the edge of the Palaeo-Agulhas Plain to the little Karoo (South Africa) in marine isotope stages 5–3 as indicated by speleothems. *Quat. Sci. Rev.* <https://doi.org/10.1016/j.quascirev.2019.06.025>.

Cerling, T.E., Harris, J.M., 1999. Carbon isotope fractionation between diet and bioapatite in ungulate mammals and implications for ecological and paleoecological studies. *Oecologia* 120, 347–363.

Cerling, T.E., Sharp, Z.D., 1996. Stable carbon and oxygen isotope analysis of fossil tooth enamel using laser ablation. *Palaeogeogr. Palaeoclimatol. Palaeoecol.* 126, 173–186. [https://doi.org/10.1016/S0031-0182\(96\)00078-8](https://doi.org/10.1016/S0031-0182(96)00078-8).

Chase, B.M., Meadows, M.E., 2007. Late Quaternary dynamics of southern Africa's winter rainfall zone. *Earth Sci. Rev.* 84, 103–138.

Codron, J., Codron, D., Lee-Thorp, J.A., Sponheimer, M., Bond, W.J., de Ruiter, D., Grant, R., 2005. Taxonomic, anatomical, and spatio-temporal variations in the stable carbon and nitrogen isotopic compositions of plants from an African savanna. *J. Archaeol. Sci.* 32, 1757–1772. <https://doi.org/10.1016/j.jas.2005.06.006>.

Copeland, S.R., Cawthra, H.C., Fisher, E.C., Lee-Thorp, J.A., Cowling, R.M., le Roux, P.J., Hodgkins, J., Marean, C.W., 2016. Strontium isotope investigation of ungulate movement patterns on the Pleistocene Palaeo-Agulhas Plain of the greater Cape Floristic region, South Africa. *Quat. Sci. Rev.* 141, 65–84. <https://doi.org/10.1016/j.quascirev.2016.04.002>.

Cowling, R., Richardson, D., 1995. *Fynbos: South Africa's Unique Floral Kingdom*. University of Cape Town, Cape Town.

Cowling, R.M., 1983. The occurrence of C_3 and C_4 grasses in fynbos and allied shrublands in the South Eastern Cape, South Africa. *Oecologia* 58, 121–127.

Cowling, S.A., Cox, P.M., Jones, C.D., Maslin, M.A., Peros, M., Spall, S.A., 2008. Simulated glacial and interglacial vegetation across Africa: implications for species phylogenies and trans-African migration of plants and animals. *Global Change Biol.* 14, 827–840.

Davies, K.C., Jarvis, J.U.M., 1986. The burrow systems and burrowing dynamics of the mole rats *Bathyergus suillus* and *Cryptomys hottentotus* in the fynbos of the south-western Cape, South Africa. *J. Zool.* 209, 125–147.

De Graaff, G., 1981. *The Rodents of Southern Africa*. Butterworths, Durban.

DeNiro, M.J., Epstein, S., 1978. Influence of diet on the distribution of carbon isotopes in animals. *Geochem. Cosmochim. Acta* 42, 495–506.

Ecker, M., Brink, J.S., Rossouw, L., Chazan, M., Horwitz, L.K., Lee-Thorp, J.A., 2018. The palaeoecological context of the Oldowan–Acheulean in southern Africa. *Nat. Ecol. Evol.* 2, 1080–1086.

Estes, R.D., 1991. *The Behavior Guide to African Mammals*. University of California Press, Berkeley.

Ewer, R.F., 1973. *The Carnivores*. Cornell University Press, Ithaca.

Fernandez-Jalvo, Y., Andrews, P., 1992. Small mammal taphonomy of Gran Dolina, Atapuerca (Burgos), Spain. *J. Archaeol. Sci.* 19, 407–428.

Fisher, E.C., Bar-Matthews, M., Jerardino, A., Marean, C.W., 2010. Middle and late Pleistocene paleoscape modeling along the southern coast of South Africa. *Quat. Sci. Rev.* 29, 1382–1398.

Franz-Odenaal, T.A., Lee-Thorp, J.A., Chinsamy, A., 2002. New evidence for the lack of C_4 grassland expansions during the early Pliocene at Langebaanweg, South Africa. *Paleobiology* 28, 378–388.

Gehler, A., Tütken, T., Pack, A., 2012. Oxygen and carbon isotope variations in a modern rodent community – implications for palaeoenvironmental reconstructions. *PLoS One* 7, e49531. <https://doi.org/10.1371/journal.pone.0049531>.

Hare, V., Sealy, J., 2013. Middle Pleistocene dynamics of southern Africa's winter rainfall zone from $\delta^{13}C$ and $\delta^{18}O$ values of Hoedjiespunt faunal enamel. *Palaeogeogr. Palaeoclimatol. Palaeoecol.* 374, 72–80.

Hare, V.J., Loftus, E., Jeffrey, A., Ramsey, C.B., 2018. Atmospheric CO₂ effect on stable carbon isotope composition of terrestrial fossil archives. *Nat. Commun.* 9, 1–8.

Hodgkins, J., le Roux, P., Marean, C.W., Penkman, K., Crisp, M., Fisher, E., Lee-Thorp, J., 2018. The role of ostrich in shaping the landscape use patterns of humans and hyenas on the southern coast of South Africa during the late Pleistocene. In: Birch, S.E.P. (Ed.), *Multispecies Archaeology*. Routledge, London, pp. 333–346.

Hodgkins, J., Marean, C.W., Venter, J., Richardson, L., Roberts, P., Zech, J., Difford, M., Copeland, S.R., Keller, H.M., Lee-Thorp, J.A., 2020. An isotopic test of the seasonal migration hypothesis for large grazing ungulates inhabiting the Palaeo-Agulhas Plain (south coast, South Africa). *Quat. Sci. Rev.* this volume In this issue.

Hopley, P.J., Latham, A.G., Marshall, J.D., 2006. Palaeoenvironments and palaeodiets of mid-Pliocene micromammals from Makapansgat Limeworks, South Africa: a stable isotope and dental microwear approach. *Palaeogeogr. Palaeoclimatol. Palaeoecol.* 233, 235–251. <https://doi.org/10.1016/j.palaeo.2005.09.011>.

Hynek, S.A., Passey, B.H., Prado, J.L., Brown, F.H., Cerling, T.E., Quade, J., 2012. Small mammal carbon isotope ecology across the Miocene–Pliocene boundary, northwestern Argentina. *Earth Planet Sci. Lett.* 321–322, 177–188. <https://doi.org/10.1016/j.epsl.2011.12.038>.

Jacobs, Z., 2010. An OSL chronology for the sedimentary deposits from Pinnacle Point Cave 13B - A punctuated presence. *J. Hum. Evol.* 59, 289–305.

Jeffrey, A., 2016. *Exploring Human Responses to Climate and Environmental Change in North Africa Using Oxygen and Carbon Stable Isotopes from Small Mammal Teeth*. Oxford University, Oxford. PhD Thesis.

Jeffrey, A., Denys, C., Stoetzel, E., Lee-Thorp, J.A., 2015. Influences on the stable oxygen and carbon isotopes in gerbillid rodent teeth in semi-arid and arid environments: implications for past climate and environmental reconstruction. *Earth Planet Sci. Lett.* 428, 84–96.

Kingdon, J., 2015. *The Kingdon Field Guide to African Mammals*. Princeton University Press, Princeton.

Kohn, M.J., Schoeninger, M.J., Valley, J.W., 1996. Herbivore tooth oxygen isotope compositions: effects of diet and physiology. *Geochem. Cosmochim. Acta* 60, 3889–3896.

Lee-Thorp, J., 2002. Two decades of progress towards understanding fossilization processes and isotopic signals in calcified tissue minerals. *Archaeometry* 44, 435–446.

Lee-Thorp, J., Talma, A.S., 2000. Stable light isotopes and environments in the southern African Quaternary and late Pliocene. In: Partridge, T.C., Maud, R.R. (Eds.), *The Cenozoic of Southern Africa*. Oxford University Press, Oxford, pp. 236–251.

Lee-Thorp, J.A., Manning, L., Sponheimer, M., 1997. Exploring problems and opportunities offered by down-scaling sample sizes for carbon isotope analyses of fossils. *Bull. Soc. Geol. France* 168, 767–773.

Lee-Thorp, J.A., Sealy, J.C., van der Merwe, N.J., 1989. Stable carbon isotope ratio

- differences between bone collagen and bone apatite, and their relationship to diet. *J. Archaeol. Sci.* 16, 585–599. [https://doi.org/10.1016/0305-4403\(89\)90024-1](https://doi.org/10.1016/0305-4403(89)90024-1).
- Leichliter, J.N., Sponheimer, M., Avenant, N.L., Sandberg, P.A., Paine, O.C.C., Codron, D., Codron, J., Passey, B.H., 2016. Small mammal insectivore stable carbon isotope compositions as habitat proxies in a South African savanna ecosystem. *J. Archaeol. Sci.: Report* 8, 335–345.
- Lindars, E.S., Grimes, S.T., Matthey, D.P., Collinson, M.E., Hooker, J.J., Jones, T.P., 2001. Phosphate $\delta^{18}O$ determination of modern rodent teeth by direct laser fluorination: an appraisal of methodology and potential application to palaeoclimate reconstruction. *Geochem. Cosmochim. Acta* 65, 2535–2548.
- Luz, B., Kolodny, Y., 1985. Oxygen isotope variations in phosphate of biogenic apatites, 1985. Mammal teeth and bones. *Earth Planet Sci. Lett.* 75, 29–36. [https://doi.org/10.1016/0012-821X\(85\)90047-0](https://doi.org/10.1016/0012-821X(85)90047-0).
- Marean, C., Nilssen, P., Brown, K., Jerardino, A., Stynder, D., 2004. Paleoanthropological investigations of Middle Stone Age sites at Pinnacle Point, Mossel Bay (South Africa): archaeology and hominid remains from the 2000 field season. *PaleoAnthropology* 5, 14–83.
- Marean, C.W., 2010. Pinnacle Point Cave 13B (Western Cape Province, South Africa) in context: The Cape Floral Kingdom, shellfish, and modern human origins. *J. Hum. Evol.* 59, 425–443. <https://doi.org/10.1016/j.jhevol.2010.07.011>.
- Marean, C.W., Cawthra, H.C., Cowling, R.M., Esler, K.J., Fisher, E., Milewski, A., Potts, A.J., Singels, E., De Vynck, J., 2014. Stone Age People in a Changing South African Greater Cape Floristic Region. In: Allsopp, N., Colville, J.F., Verboom, T. (Eds.), *Fynbos: Ecology, Evolution, and Conservation of a Megadiverse Region*. Oxford University Press, Oxford, pp. 164–199.
- Matthews, T., n.d. A Summary of the Micromammal Population from PP30 (Brown hyaena den).
- Matthews, T., 2004. The Taxonomy and Taphonomy of Mio-Pliocene and Late Middle Pleistocene Micromammals from the Cape West Coast, South Africa. Ph.D Thesis. University of Cape Town, South Africa.
- Matthews, T., Marean, C.W., Cleghorn, N., 2019. Past and present distributions and community evolution of Muridae and Soricidae from MIS 9 to MIS 1 on the edge of the Palaeo-Agulhas Plain (south coast, South Africa). *Quat. Sci. Rev.* <https://doi.org/10.1016/j.quascirev.2019.05.026>.
- Matthews, T., Marean, C.W., Nilssen, P.J., 2009. Micromammals from the Middle Stone Age (92–167 ka) at cave PP13B, Pinnacle Point, south coast, South Africa. *Paleontologia Africana* 44, 112–120.
- Matthews, T., Rector, A., Jacobs, Z., Herries, A.I.R., Marean, C.W., 2011. Environmental implications of micromammals accumulated close to the MIS 6 to MIS 5 transition at Pinnacle Point cave 9 (Mossel Bay, western Cape Province, South Africa). *Palaeogeogr. Palaeoclimatol. Palaeoecol.* 302, 213–229.
- Mills, M.G.L., 1990. Kalahari Hyaenas: the Comparative Behavioural Ecology of Two Species. Unwin Hyman, London.
- Muller, M.J., Tyson, P.D., 1988. Winter rainfall over the interior of South Africa during extreme dry years. *S. Afr. Geogr. J.* 70, 20–30.
- Oestmo, S., Marean, C.W., 2014. Pinnacle Point: excavation and survey methods. In: Smith, C. (Ed.), *Encyclopedia of Global Archaeology*. Springer, New York, pp. 5955–5959.
- Passey, B.H., Cerling, T.E., 2006. In situ stable isotope analysis ($\delta^{13}C$, $\delta^{18}O$) of very small teeth using laser ablation GC/IRMS. *Chem. Geol.* 235, 238–249. <https://doi.org/10.1016/j.chemgeo.2006.07.002>.
- Passey, B.H., Robinson, T.F., Ayliffe, L.K., Cerling, T.E., Sponheimer, M., Dearing, M.D., Roeder, B.L., Ehleringer, J.R., 2005. Carbon isotope fractionation between diet, breath CO_2 , and bioapatite in different mammals. *J. Archaeol. Sci.* 32, 1459–1470.
- Podlesak, D.W., Torregrossa, A.-M., Ehleringer, J.R., Dearing, M.D., Passey, B.H., Cerling, T.E., 2008. Turnover of oxygen and hydrogen isotopes in the body water, CO_2 , hair, and enamel of a small mammal. *Geochem. Cosmochim. Acta* 72, 19–35.
- Reason, C., Rouault, M., 2005. Links between the Antarctic Oscillation and winter rainfall over western South Africa. *Geophys. Res. Lett.* 32, L07705.
- Rector, A.L., Reed, K.E., 2010. Middle and late Pleistocene faunas of Pinnacle Point and their paleoecological implications. *J. Hum. Evol.* 59, 340–357.
- Richards, M., Harvati, K., Grimes, V., Smith, C., Smith, T., Hublin, J.-J., Karkanas, P., Panagopoulou, E., 2008. Strontium isotope evidence of Neanderthal mobility at the site of Lakonis, Greece using laser-ablation PIMMS. *J. Archaeol. Sci.* 35, 1251–1256. <https://doi.org/10.1016/j.jas.2007.08.018>.
- Scholz, C.A., Johnson, T.C., Cohen, A.S., King, J.W., Peck, J.A., Overpeck, J.T., Talbot, M.R., Brown, E.T., Kalinidekafu, L., Amoako, P.Y.O., Lyons, R.P., Shanahan, T.M., Castaneda, I.S., Heil, C.W., Forman, S.L., McHargue, L.R., Beuning, K.R., Gomez, J., Pierson, J., 2007. East African megadroughts between 135 and 75 thousand years ago and bearing on early-modern human origins. In: *Proceedings of the National Academy of Sciences*, 104. *Proceedings of the National Academy of Sciences*, pp. 16416–16421, 0703874104. <https://doi.org/10.1073/pnas.0703874104>.
- Schreiner, C., Rödder, D., Measey, G.J., 2013. Using modern models to test Poynton's predictions. *Afr. J. Herpetol.* 62, 49–62. <https://doi.org/10.1080/21564574.2013.794865>.
- Sharp, Z.D., Cerling, T.E., 1996. A laser GC-IRMS technique for in situ stable isotope analyses of carbonates and phosphates. *Geochem. Cosmochim. Acta* 60, 2909–2916. [https://doi.org/10.1016/0016-7037\(96\)00128-7](https://doi.org/10.1016/0016-7037(96)00128-7).
- Skinner, J.D., Chimimba, C.T., 2005. *The Mammals of the Southern African Sub-region*. Cambridge University Press, Cambridge.
- Skinner, J.D., Haupt, M.A., Hoffmann, M., Dott, H.M., 1998. Bone collecting by Brown Hyaenas (*Hyaena brunnea*) in the Namib desert: rate of accumulation. *J. Archaeol. Sci.* 25, 69–71.
- Skinner, J.D., Van Aarde, R.J., 1991. Bone collecting by brown hyaenas (*Hyaena brunnea*) in the central Namib Desert, Namibia. *J. Archaeol. Sci.* 18, 513–523.
- Smith, B.N., Epstein, S., 1971. Two categories of $^{13}C/^{12}C$ ratios for higher plants 1. *Plant Physiol.* 47, 380–384.
- Sponheimer, M., Lee-Thorp, J.A., 1999. Oxygen isotopes in enamel carbonate and their ecological significance. *J. Archaeol. Sci.* 26, 723–728.
- Sponheimer, M., Lee-Thorp, J.A., 2001. The oxygen isotope composition of mammalian enamel carbonate from Morea Estate, South Africa. *Oecologia* 126, 153–157. <https://doi.org/10.1007/s004420000498>.
- Sponheimer, M., Lee-Thorp, J.A., 2003. Using carbon isotope data of fossil bovid communities for palaeoenvironmental reconstruction. *South Afr. J. Sci.* 99, 273–275.
- Sponheimer, M., Lee-Thorp, J.A., DeRuiter, D.J., Smith, J.M., van der Merwe, N.J., Reed, K., Grant, C.C., Ayliffe, L.K., Robinson, T.F., Heidelberg, C., 2003. Diets of southern African Bovidae: stable isotope evidence. *J. Mammal.* 84, 471–479.
- Stuut, J.B., Crosta, X., van der Borg, K., Schneider, R., 2004. Relationship between Antarctic sea ice and southwest African climate during the late Quaternary. *Geology* 32, 909–912.
- Thackeray, J.F., van der Venter, A., Lee-Thorp, J., Chimimba, C.T., van Heerden, J., 2008. Stable carbon isotope analysis of modern and fossil samples of the South African rodent *Aethomys namaquensis*. *Ann. Transvaal Mus.* 40, 43–46.
- Thorp, J.L., Van Der Merwe, N.J., 1987. Carbon isotope analysis of fossil bone apatite. *South Afr. J. Sci.* 83, 712–715.
- Tyson, P.D., 1999. Atmospheric circulation changes and paleoclimates of southern Africa. *South Afr. J. Sci.* 95, 194–201.
- Vogel, J.C., Fuls, A., Ellis, R.P., 1978. The geographical distribution of Kranz grasses in South Africa. *South Afr. J. Sci.* 74, 209–215.
- Wiesel, I., 2006. *Predatory and Foraging Behaviour of Brown Hyenas (Parahyaena brunnea (Thunberg, 1820)) at Cape Fur Seal (Arctocephalus pusillus pusillus Schreber, 1776) Colonies*. University of Hamburg. Ph.D Thesis.
- Williams, H.M., 2015. *Stable Isotope Analysis of Archaeological and Modern Micromammals from the Greater Cape Floristic Region Near Pinnacle Point, on the South Coast of South Africa*. School of Human Evolution and Social Change. Arizona State University. Ph.D Thesis.
- Yeakel, J.D., Bennett, N.C., Koch, P.L., Dominy, N.J., 2007a. The isotopic ecology of African mole rats informs hypotheses on the evolution of human diet. In: *Proceedings of the Royal Society B: Biological Sciences*, vol. 274, pp. 1723–1730. <https://doi.org/10.1098/rspb.2007.0330>.
- Yeakel, J.D., Bennett, N.C., Koch, P.L., Dominy, N.J., 2007b. The isotopic ecology of African mole rats informs hypotheses on the evolution of human diet, 274, 1723–1730.